

Intraflagellar transport proteins in ciliogenesis of photoreceptor cells

Tina Sedmak¹ and Uwe Wolfrum²

Department of Cell and Matrix Biology, Institute of Zoology, Johannes Gutenberg University, Mainz, Germany

Background information. The assembly and maintenance of cilia depend on IFT (intraflagellar transport) mediated by molecular motors and their interplay with IFT proteins. Here, we have analysed the involvement of IFT proteins in the ciliogenesis of mammalian photoreceptor cilia.

Results. Electron microscopy revealed that ciliogenesis in mouse photoreceptor cells follows an intracellular ciliogenesis pathway, divided into six distinct stages. The first stages are characterized by electron-dense centriolar satellites and a ciliary vesicle, whereas the formations of the ciliary shaft and the light-sensitive outer segment discs are features of the later stages. IFT proteins were associated with ciliary apparatus during all stages of photoreceptor cell development.

Conclusions. Our data conclusively provide evidence for the participation of IFT proteins in photoreceptor cell ciliogenesis, including the formation of the ciliary vesicle and the elongation of the primary cilium. In advanced stages of ciliogenesis the ciliary localization of IFT proteins indicates a role in IFT as is seen in mature cilia. A prominent accumulation of IFT proteins in the periciliary cytoplasm at the base of the cilia in these stages most probably resembles a reserve pool of IFT molecules for further delivery into the growing ciliary shaft and their subsequent function in IFT. Nevertheless, the cytoplasmic localization of IFT proteins in the absence of a ciliary shaft in early stages of ciliogenesis may indicate roles of IFT proteins beyond their well-established function for IFT in mature cilia and flagella.

Introduction

Cilia are highly conserved thin finger-like organelles emerging from the surface of eukaryotic cells. They are structurally divided into sub-compartments, predominantly into an axoneme and a transition zone, which emerge from the basal body complex. Cilia have multiple functions in both mature and developing organisms: for example locomotion or specific sensory function. Disruption of cilia has been associated with numerous ciliopathies, for example complex syndromes involving cystic kidneys, obesity, mental retardation, deafness, blindness and various developmental malformations (Badano et al., 2006;

Baker and Beales, 2009; Gerdes et al., 2009; Goetz and Anderson, 2010).

Cilia are formed by the mother centriole of the centrosome, which matures into the basal body and nucleates the nine microtubule doublets of the axoneme. Sorokin's pioneering studies on ciliogenesis in the 1960s revealed two principally different pathways of ciliogenesis (Sorokin, 1962, 1968), which were recently referred to as the extracellular and intracellular pathways of ciliogenesis (Molla-Herman et al., 2010; Ghossoub et al., 2011). In the extracellular ciliogenesis pathway, the mother centriole directly docks at the plasma membrane from where the ciliary shaft is formed and grows towards the extracellular environment. During intracellular ciliogenesis, the mother centriole docks to the membrane of an intracellular primary ciliary vesicle, and the cilium is assembled within the ciliary vesicle. After docking and fusion of the elongated intracellular ciliary vesicle with the plasma membrane, the ciliary shaft is released into the extracellular space.

¹Present address: Department of Biology, Animal Physiology, University of Erlangen-Nuremberg, D-91058 Erlangen, Germany.

²To whom correspondence should be addressed (email wolfrum@uni-mainz.de).

Key words: cilia, ciliogenesis, intracellular membrane trafficking, intraflagellar transport (IFT), photoreceptor cell.

Abbreviations used: CEP290, centrosomal protein 290; DAPI, 4',6-diamidino-2-phenylindole; IFT, intraflagellar transport; PNO, postnatal day 0 etc.

Assembly and maintenance of cilia require IFT (intraflagellar transport), a conserved process mediated by molecular motors and IFT particles (Rosenbaum and Witman, 2002; Pedersen and Rosenbaum, 2008). IFT comprises the bidirectional transport of IFT particles containing ciliary or flagellar cargo along the outer doublet microtubules of the axoneme. IFT particles themselves are composed of individual IFT proteins organized into the two sub-complexes A and B, suggested to participate in anterograde and retrograde IFT respectively (Cole et al., 1998; Cole, 2003; Krock et al., 2009). IFT proteins are conserved among green algae, nematodes and vertebrates. Mutations in genes encoding IFT proteins prevent ciliary assembly in all organisms investigated (Cole et al., 1998; Murcia et al., 2000; Pazour et al., 2002; Tsujikawa and Malicki 2004; Krock and Perkins, 2008; Omori et al., 2008). From these genetic data there is no doubt that IFT is essential for the development of cilia. However, only little substantial data are available on the role of IFT and the specific functions of the individual IFT proteins during ciliogenesis (Pedersen et al., 2008; Sukumaran and Perkins, 2009). This insufficiency is partly due to the deficient knowledge of the specific sub-cellular localization of the IFT components, particularly individual IFT proteins during ciliogenesis. Here we systematically analyse the expression and sub-cellular localization of four different IFT-complex B proteins, namely IFT20, IFT52, IFT57 and IFT88, as well as the IFT-complex A protein IFT140, during ciliogenesis in rod photoreceptor cells by a combination of high-resolution immunofluorescence and electron microscopy.

We have recently introduced the vertebrate retina and its photoreceptor cells as a useful model system to verify the roles of individual IFT proteins through their sub-cellular localization (Sedmak and Wolfrum, 2010). Photoreceptor cells are highly polarized sensory neurons organized in morphological and functional distinct cellular compartments. The photosensitive outer segment of vertebrate cone and rod photoreceptor cells is a drastically evolutionarily modified primary cilium (Besharse and Horst, 1990; Roepman and Wolfrum, 2007; Pazour and Bloodgood, 2008) that contains all components of the visual transduction cascade, which in rod cells are arranged at hundreds of flattened membrane discs separated from the plasma membrane (Sung and

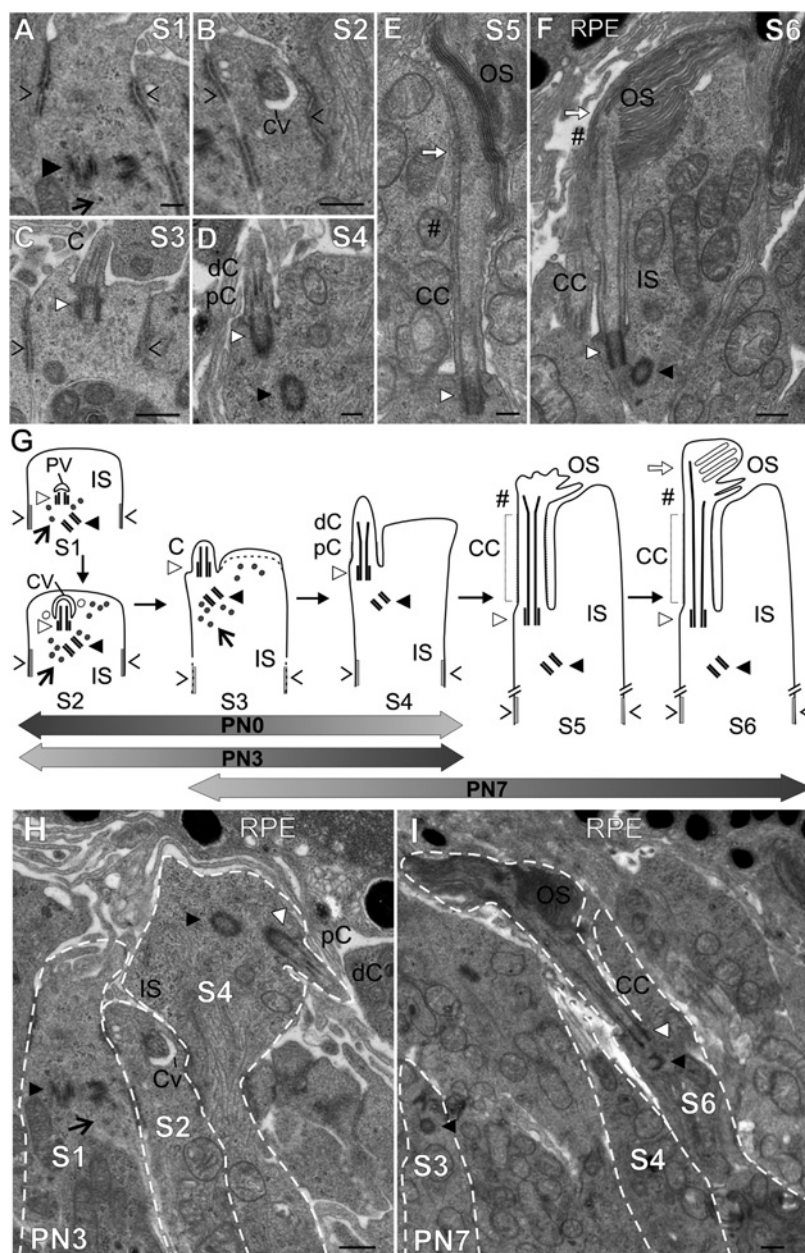
Chuang, 2010). The outer segment is linked to the inner segment containing all the organelles necessary for biosynthesis by the connecting cilium, a slightly modified and extended transition zone of a prototypic cilium (Roepman and Wolfrum, 2007). The axon projects from the photoreceptor cell body to the synaptic terminus connecting the photoreceptor cells with the secondary retinal neurons (tom Dieck and Brandstätter, 2006).

During the development of the vertebrate retina, photoreceptor cells mature from precursors present in the outer neuroblastic layer (Livesey and Cepko, 2001). In rodents, the retina is rod-dominated and cones constitute only ~3% of the total photoreceptors in wild-type mice (Carter-Dawson and LaVail, 1979; Jeon et al., 1998). In mice the rod photoreceptor differentiation starts postnatally and ciliogenesis of fully mature outer segments lasts over 2 weeks (LaVail, 1973). The ciliogenesis of rod cells is not completely synchronized throughout development (Tokuyasu and Yamada, 1959; Greiner et al., 1981; Nir et al., 1984; Chaitin, 1992; Sung and Chuang, 2010) and therefore different stages of developing photoreceptor cilia can be analysed in parallel, offering a useful system to study primary cilia's assembly. However, there are controversial data on the ciliogenesis pathway of rod photoreceptor cells in the literature. Although recent reviews indicated that mammalian photoreceptor cilia develop via an extracellular pathway (Sung and Chuang, 2010; Ghossoub et al., 2011), an electron microscopy analysis has implicated the intracellular pathway (Greiner et al., 1981). This evident discrepancy has prompted us to investigate ciliogenesis in photoreceptor cells in a more detailed reanalysis.

In the present study we demonstrate that ciliogenesis in photoreceptor cells occurs via the intracellular pathway. Furthermore, dissection into various developmental stages has allowed us to analyse the spatial distribution of individual IFT proteins at the diverse stages of ciliogenesis. We show that IFT proteins are present at all stages of the intracellular ciliogenesis of photoreceptor cells. These results provide evidence for a role of IFT proteins in ciliogenesis even before the IFT motility system starts to transport cargo along the axonemal microtubules, which may suggest putative functions of IFT proteins independent of IFT.

Figure 1 | Different stages of photoreceptor cell ciliogenesis

(A–F) Electron micrographs of different stages of photoreceptor cell ciliogenesis in PN0, PN3 and PN7 mouse retinas schematically illustrated in (G). S1: the mother centriole (white arrowhead), the daughter centriole (black arrowhead) and electron-dense centriolar satellites (black arrow) are present in the cytoplasm of differentiating photoreceptors. The distal end of the mother centriole is enclosed by the primary vesicle (PV). S2: the ciliary bud elongates to the ciliary shaft and the mother centriole matures to the basal body. S3: the flattened PV is enlarged by repeated fusion of post-Golgi vesicles forming the ciliary vesicle (CV). CV fuses with the plasma membrane of the inner segment (IS), and the newly assembling cilium (C) appears on the cell surface. S4: the elongating cilium is divided into the proximal cilium (pC), characterized by periodic bead-like densities in the plasma membrane distal cilium (dC) which are absent in the distal cilium (dC). S5: pC becomes the connecting cilium (CC), the dC forms the outer segment (OS). S6: axoneme (white arrow) prolongs into the OS in which first stacks of membrane discs appear. Grey circles indicated by the black arrow represent electron-dense granules of centriolar satellites. In S3 the dotted line indicates



elongation and morphological remodelling of apical IS during development. Symbols '>' and '<' indicate adherent junctions at the outer limiting membrane. (H, I) Electron micrographs demonstrating the non-synchronized photoreceptor cell ciliogenesis in PN3 and PN7 mouse retinas indicated by arrowbars in (G). Defined stages of ciliogenesis are encircled by broken lines. RPE, retinal pigment epithelium. Scale bars: (A, B, D, E, H) 200 nm and (C, F, I) 400 nm.

Results

Ultrastructural analysis of the ciliogenesis in differentiating photoreceptor cells

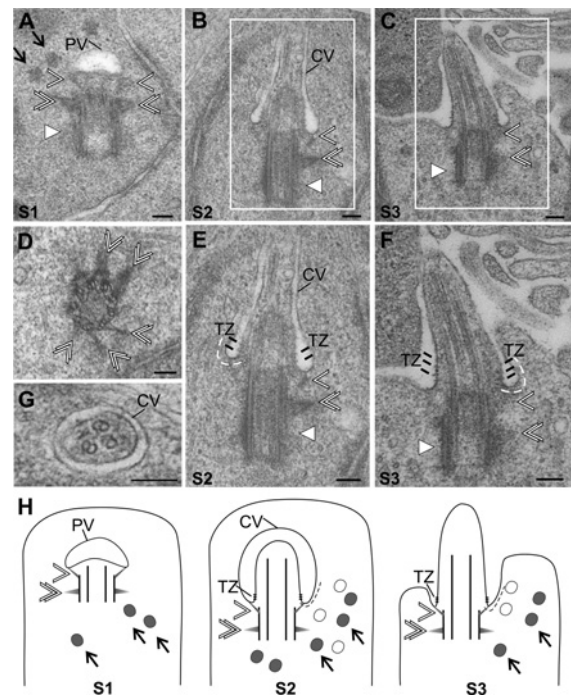
The ciliogenesis in photoreceptor cells was analysed in retinas of mice at PN0 (postnatal day 0), PN3 and PN7 by conventional transmission electron microscopy (Figure 1). The photoreceptor cells differentiate in the apical part of the neuroblastic layer of the developing mouse retina. Ciliogenesis in the differentiating photoreceptor cells is not synchronized (Figures 1H and 1I). For the nomenclature of the different stages of ciliogenesis in photoreceptor cells, we follow Pedersen et al. (2008), who proposed four stages for primary cilia and we added two photoreceptor-specific stages, S5 and S6, characteristic of the outer segment formation. In retinas of PN0 and PN3 mice, we observed photoreceptor cells in stages S1–S4 (Figure 1H), whereas in PN7 stages S3–S6 of ciliogenesis were predominant (Figure 1I).

In stage S1 of the photoreceptor cell ciliogenesis, an intracellular primary ciliary vesicle appears at the distal end of the mother centriole. During S1 the mother centriole matures into the basal body and two sets of accessory structures, the distal and sub-distal appendages, appear at the distal part of the basal body (Figure 2). The distal appendages project to the membrane of the primary vesicle, whereas the sub-distal appendages protrude from the basal body into the pericentriolar cytoplasm. These appendages are absent from the daughter and the adjacent centriole.

In stages S1–S3 of the differentiating photoreceptor cells, we observed electron-dense spherical granules, the centriolar satellites in the cytoplasm of the periciliary region of the evolving photoreceptor cilium (Figures 2A and 2H). The number of centriolar satellites gradually decreases from S1 to S3 until they disappear in S4. They are non-membranous cytoplasmic granules that are believed to be involved in the transport of ciliary and centriolar proteins, for example centrin, pericentrin and ninein, to the basal body (Kubo et al., 1999; Laoukili et al., 2000; Dammermann and Merdes, 2002; Hames et al., 2005).

Figure 2 | Structural features of early photoreceptor cell ciliogenesis

(A–G) Electron micrograph of the differentiating centriolar appendages and satellites schematically illustrated in (H). (A, B) In S1–S2 distal (single white open arrowhead) and sub-distal (white open double arrowhead) accessory appendages are present before the cilium appears at the cell surface in S3. Centriolar satellites (black arrow) are organized near the basal body (white arrowhead). (B, C, E, F) These panels demonstrate periodic bead-like densities of the plasma membrane (black lines), which are characteristic of the transition zone (TZ) appearing at the proximal cilium and ciliary pocket (broken line) in S2 and S3. (E, F) Magnified images of (B, C). (D) Cross-section through the basal body and sub-distal appendages (white open double arrowhead). (G) Cross-section through the axoneme of elongating ciliary shaft enclosed by the membrane of ciliary vesicle (CV). PV, primary CV. Scale bars: 100 nm.



In stage S2 the ciliary bud emerges from the distal basal body, elongates and forms the ciliary shaft, which projects into the growing ciliary vesicle

Figure 3 | IFT57 expression in the developing mouse retina

(A, F) DAPI staining of the nuclear DNA in PN0 and PN21 mouse retina respectively. (B–E) Indirect immunofluorescence of antibodies against IFT57 at PN0, PN3, PN7 and PN21 (mature) retinas. At PN0 and PN3 IFT57 is detected as a dotted pattern in the apical region of the neuroblastic layer (NBL). At PN7 and PN21 retinas, IFT57 is localized in the region between the photoreceptor cell outer segment (OS) and the inner segment (IS), where the connecting cilium (CC; double white arrowhead) is present. In addition scattered dots are stained in the proximal region of the NBL in PN0 and PN3 retinas and in the outer plexiform layer (OPL; white asterisk) of PN7 and mature retinas, where the synapse between the photoreceptor cells and secondary neurons (2nd) are present. (G) Schema of a rod photoreceptor cell and its connection to 2nd. RPE, retinal pigment epithelium; black asterisk, apical IS; N, photoreceptor nuclei in the outer nuclear layer (ONL). Scale bars: 10 μ m.

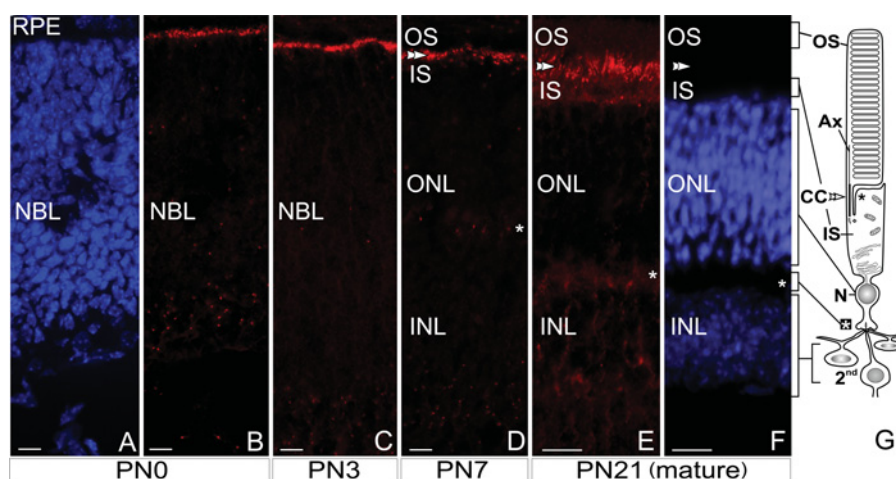


(Figure 2). The primary ciliary vesicle expands by the fusion of post-Golgi vesicles to form the so-called ciliary vesicle. At this stage a small ciliary pocket appears at the base of the ciliary shaft (Figures 2B and 2E). Periodic bead-like densities that are characteristic of the plasma membrane of the transition zone (Gilula and Satir, 1972; Besharse and Horst, 1990) become apparent in the proximal cilium in stage S2 (Figures 2B and 2C). As the cilia continue to mature, the transition zone extends to form the connecting cilium of the mature photoreceptor cell (Figures 1E–1G and 1I and Figures 2C and 2F). The ciliary vesicle fuses with the plasma membrane, and from stage S3 onwards the cilium is exposed at the surface of the photoreceptor cell (Figures 1C, 1G and 2C, 2F). In conclusion, the early stages of ciliogenesis (S1–S3) in photoreceptor cells exhibit the characteristic hallmarks of an intracellular ciliogenesis pathway (Molla-Herman et al., 2010; Ghossoub et al., 2011).

In stage S4 the distal part of the evolving cilium begins to swell and internal membrane vesicles or tubules appear. These membrane structures fuse to form the disc membranes of the rod outer seg-

ment in stage S5 (Figure 1E). From stage S6 onwards, stacks of outer segment discs can be identified that still lack the characteristic organization of the mature outer segments (Figures 1F and 1G). It is notable that, during ciliogenesis, the polarity of the photoreceptor cilia differs and evolving cilia can point with their tips either to the outer limiting membrane or to the retinal pigment epithelium (Figure 1H).

Expression of individual IFT proteins in the developing mouse retina

Indirect immunofluorescence analyses of developing mouse retinas at PN0, PN3 and PN7 revealed that the IFT proteins IFT20, IFT52, IFT57, IFT88 and IFT140 are expressed during all developmental stages of the retina (Figure 3; see Supplementary Figure S1 available at: <http://www.biolcell.org/boc/103/boc1030449add.htm>). The staining patterns of all anti-IFT antibodies applied in the present study were very similar. As an example we show anti-IFT57 labelling of retinal cryosections in Figure 3. In PN0 and PN3 mouse retinas, IFT

proteins were concentrated in the apical region of the neuroblastic layer proximal to the retinal pigment epithelium (Figures 3A–3C). Weaker immunofluorescence was observed in the cytoplasm of the cells of the entire neuroblastic layer. At PN7 the characteristic neuronal layers of the vertebrate retina became apparent and the IFT distribution was similar to IFT staining in mature retinas (Figures 3D and 3E; Supplementary Figure S1C; Sedmak and Wolfrum, 2010).

IFT proteins are associated with evolving ciliary structures in developing photoreceptor cells at all stages

To elucidate the sub-cellular localization of individual IFT proteins in the differentiating cilium of photoreceptor cells, cryosections of postnatal retinas (PN0, PN3, PN7 and mature PN21) were analysed by double labelling with antibodies against IFT proteins and against centrin, a marker for the connecting cilium, the basal body and the associated centriole (Trojan et al., 2008). This co-labelling allowed us to determine the spatial localization of IFT proteins in the photoreceptor ciliary apparatus by immunofluorescence microscopy (Figure 4; see also Supplementary Figure S2 available at: <http://www.biolcell.org/boc/103/boc1030449add.htm>). High-resolution immunofluorescence analyses of double-labelled specimens revealed that, in the early stages S1–S4 of photoreceptor cell ciliogenesis, IFT proteins were partly co-localized with centrin, indicating IFT localization in the mother centriole or basal body, as well as with the elongating ciliary bud and the adjacent daughter centriole (Figure 4; Supplementary Figure S2). The stages of photoreceptor ciliogenesis were scored according to the length of the differentiating connecting cilium. Subsequently, during the differentiating stages S5 and S6 the sub-ciliary distribution pattern of the IFT proteins resembled the localization recently described for the mature photoreceptor cell (Figure 4; Supplementary Figure S2; Sedmak and Wolfrum, 2010). IFT52, IFT57, IFT88 and IFT140 were most concentrated at the border of the anti-centrin positive connecting cilium at the base of the outer segment. These molecules were also detectable along the shaft and in the proximal part of the connecting cilium. In contrast with the other IFT proteins analysed, IFT20

was only detected in the basal part of the connecting cilium and at the distal region of the adjacent centriole.

To elucidate the sub-cellular localization of IFT molecules during photoreceptor ciliogenesis in more detail, immunoelectron microscopy was performed using antibodies against IFT proteins in PN0, PN3 and PN7 mouse retinas. During the early ciliogenesis stages S1–S2, all investigated IFT proteins were associated with the daughter centriole and the mother centriole or with the basal body (S2; Figure 5). At the basal body they were present in the distal and sub-distal centriolar appendages (Figures 6A–6C, 6E and 6F). In stages S2–S3 the IFT proteins were additionally found in the cytoplasm of the differentiating photoreceptor cells, at the centriolar satellites (Figures 6, 7 and 8) and associated with non-ciliary vesicular structures, putative post-Golgi vesicles (Figure 7). In the periciliary cytoplasm these vesicles were present close to the mother centriole/basal body and, with the exception of IFT88 in the vicinity of the ciliary vesicle or at the vesicle membrane, possibly frozen in the fusion process (Figure 7A and 7A'). IFT20 was also found at membrane stacks of the Golgi apparatus in differentiating photoreceptor inner segments, which was confirmed by double immunofluorescence labelling using the Golgi resident marker anti-GM130 (see Supplementary Figure S3 available at <http://www.biolcell.org/boc/103/boc1030449add.htm>).

In addition to their basal body localization, we detected IFT52, IFT57, IFT88 and IFT140 in the evolving ciliary shaft for the first time (in stage S3; Figure 8). In the subsequent stages of ciliogenesis these IFT proteins were found in the proximal cilium and the distal cilium, characteristic of stage S4, and the connecting cilium, from stage S5 onwards (Figures 4, 7 and 9; Supplementary Figure S2). Immunoelectron microscopy analyses of stages S5 and S6 of photoreceptor ciliogenesis revealed the highest concentration of IFT52, IFT57, IFT88 and IFT140 at the base of the outer segment (Figure 9). In addition, immunolabelling of IFT88 and IFT140 was detected in the axoneme which projects into the evolving outer segment in stage S6 of photoreceptor ciliogenesis (Figures 9D–9G).

In contrast with other IFT proteins, IFT20 was absent from the ciliary shaft and the connecting cilium in stages S4 and S5 respectively (Figures 4,

Figure 4 | Localization of IFT20, IFT57 and IFT88 during ciliogenesis in retinal photoreceptor cells

(A–D) Images of indirect immunofluorescence labelling with antibodies to IFT proteins (red) in cryosections through developing PN0, PN3, PN7 and mature (PN21) mouse retinas. (A'–D') Merged images of double immunofluorescence of anti-IFT (red) and anti-centrin (green) antibodies. Cen is applied as a marker for the connecting cilia, the basal body (white triangle) and the adjacent centriole (black triangle). (A''–D'') Scheme of ciliary localization of IFT proteins (red) in relation to Cen (green) during ciliogenesis. The photoreceptor cell ciliogenesis is not synchronized. Different stages of ciliogenesis (S1–S6) are present in parallel in PN0, PN3 and PN7 mouse retinas. In stages S1–S4 of ciliogenesis double labelling reveals identical staining pattern of all IFT proteins partially co-localizing with Cen at the basal body and adjacent centriole. In S5, S6 (S5/6) and in the mature cilium, IFT proteins are differentially located: all three IFT proteins associate with the basal body at the base of the cilium (C) and connecting cilium (CC). IFT20 is additionally found at the adjacent centriole (black triangle), but is not detectable in the CC. The labelling of IFT88 extends into the axoneme (white arrow). Symbols '>' and '<', adherent junctions at the outer limiting membrane; IS, inner segment; OS, outer segment; #, base of the OS. Scale bars: (A'–C') 0.125 μm and (D') 0.5 μm.

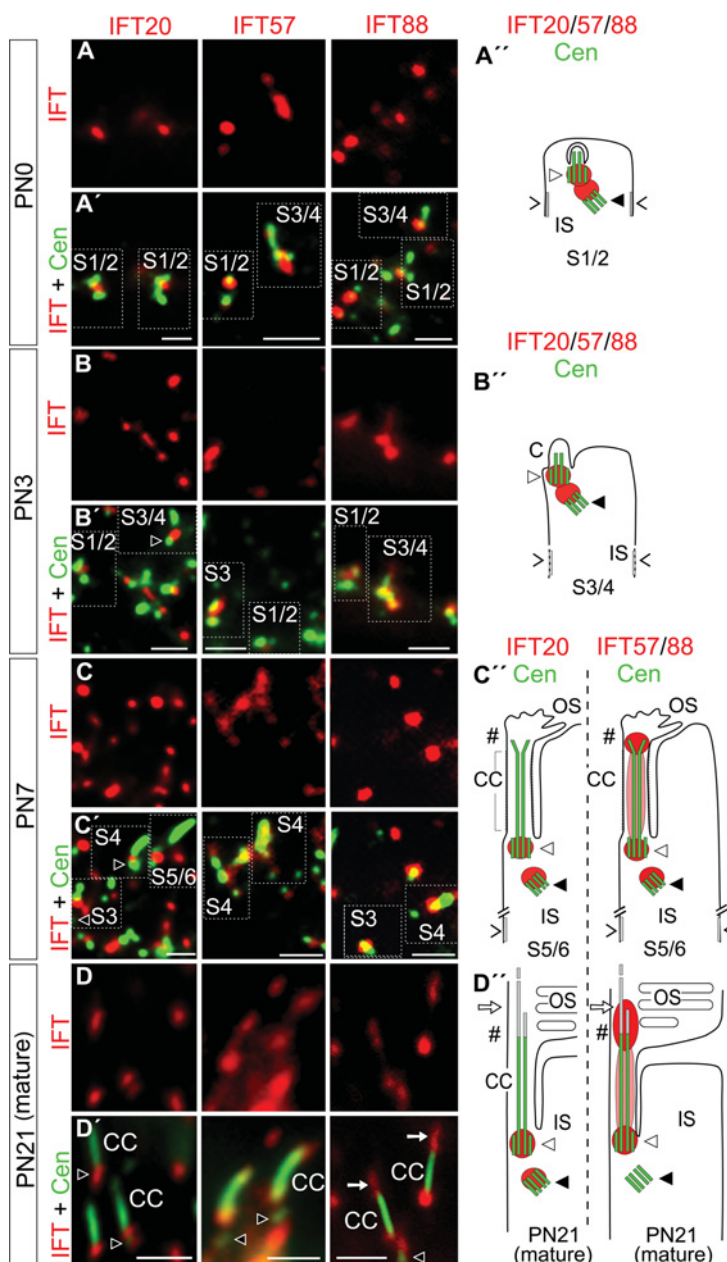
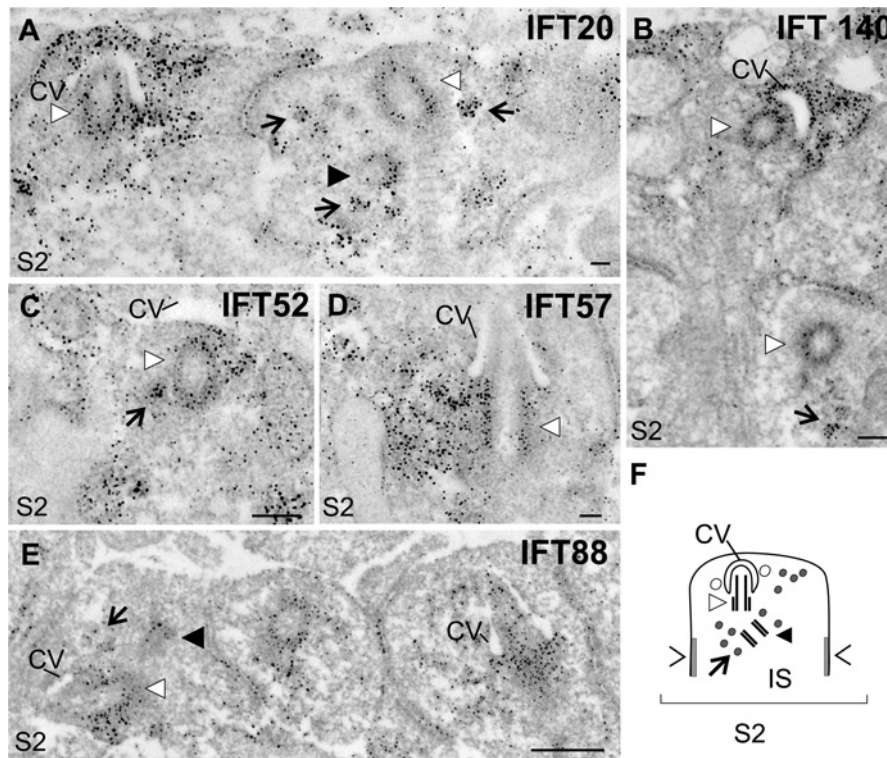


Figure 5 | IFT proteins associated with ciliary structures and in the cytoplasm at stage S2 of photoreceptor cell ciliogenesis

(A–E) Electronmicrographs of anti-IFT20, IFT52, IFT57, IFT88 and IFT140 immunolabelling, showing parts of differentiating mouse photoreceptor cells. In stage S2 of ciliogenesis, IFT20, IFT52, IFT57, IFT88 and IFT140 are localized at the mother centrioles (white arrowhead) of forming photoreceptor cilia, at daughter centriole (black arrowhead) and in the cytoplasm, where they are associated with centriolar satellites (electron-dense granules; black arrow and grey circles in F). (A, B) In addition to their localization at the mother centriole, IFT20 and IFT140 are concentrated around the ciliary vesicle (CV) and in the inner segment (IS) cytoplasm. (F) Diagram of a photoreceptor cell in stage S2 of ciliogenesis. Symbols '>' and '<', adherent junctions at the outer limiting membrane. Scale bars: (A, B, D) 100 nm, (C) 200 nm and (E) 400 nm.



8 and 10; Supplementary Figure S2), which resembles the mature situation (Figure 10H; Sedmak and Wolfrum, 2010). However, we detected IFT20 during the transition of stages S4 to S5/S6 at the base of the evolving rod outer segments (Figure 10; Supplementary Figure S3). Nevertheless, we were not able to find IFT20 in connecting cilia and outer segments of mature photoreceptor cells, confirming our previous data (Figure 10H; Sedmak and Wolfrum, 2010).

Supplementary data

Supplementary Figure S1 presents the expression of IFT proteins in the developing mouse retina using

immunofluorescence analyses. Supplementary Figure S2 demonstrates the spatial distribution of IFT52 and IFT140 proteins during ciliogenesis of retinal photoreceptor cells. Supplementary Figure S3 shows sub-cellular localization of IFT20 at the Golgi apparatus and in the cilium of differentiating mouse photoreceptor cells.

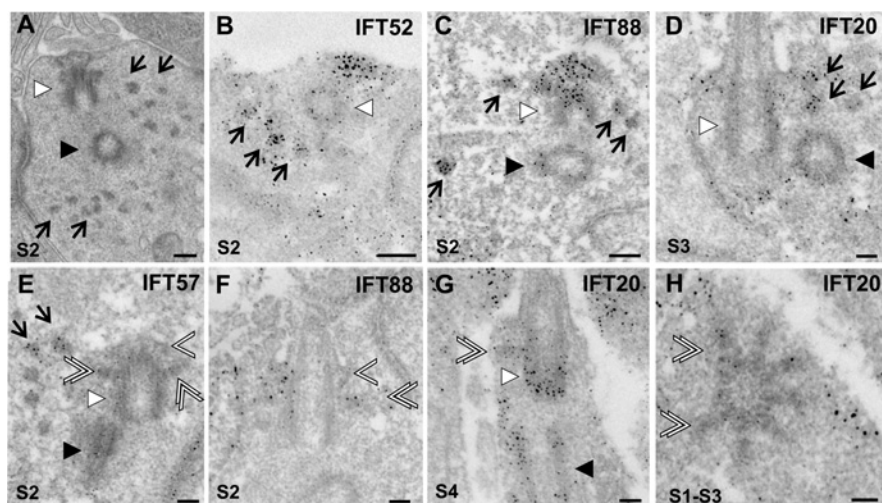
Discussion

Photoreceptor cilia development follows an intracellular ciliogenesis pathway

In the present study we have reinvestigated the ciliogenesis pathway in rod photoreceptor cells

Figure 6 | Association of IFT proteins with centriolar satellites and appendages during early ciliogenesis

(A, E) Conventional electron micrograph of the basal body region during early ciliogenesis in stage S2. (B–C, E, F, H) Immunoelectron labelling of IFT20, IFT52, IFT57 and IFT88 in early stages of photoreceptor ciliogenesis. (D–H) In stage S2, centriolar satellites (black arrows) accumulate around the basal body (white arrowhead) and the adjacent centriole (black arrowhead), but in S3 (D) the number of centriolar satellites is reduced, and they move more apically to the apical inner segment. IFT20, IFT57 and IFT88 proteins are localized at the distal (single white open arrowhead) and sub-distal (white double open arrowhead) accessory appendages. Scale bars: (A–C) 200 nm and (D–H) 100 nm.



for the clarification of controversial data reported previously (Sung and Chuang, 2010; Ghossoub et al., 2011). Our results revealed that the photoreceptor ciliogenesis in mammalian retinas follows the intracellular ciliogenesis pathway previously hypothesized by Greiner et al. (1981). This intracellular ciliogenesis pathway is characteristic of not only fibroblasts and RPE1 cells, but also neurons (Molla-Herman et al., 2010). Moreover, our analyses revealed that photoreceptor ciliogenesis can, in principle, be divided into the same stages previously described for cell types with intracellular ciliogenesis (Sorokin, 1962; Pedersen et al., 2008). During the early stages of ciliogenesis, the mother centriole matures into the basal body in the cytoplasm of the differentiating photoreceptor cell, docking with its appendages to the membrane of the intracellular primary ciliary vesicle. The close relation of cytoplasmic vesicles, most probably post-Golgi vesicles, to the ciliary vesicle (e.g. Figures 2 and 7) indicates that the ciliary vesicle is fed by post-Golgi vesicles, which confirm Sorokin's findings in fibroblasts and smooth muscle cells (Sorokin, 1962). In contrast, we did not find any indications for an endocytotic origin of the cili-

ary vesicle as previously suggested (Kim et al., 2010; Molla-Herman et al., 2010; Rattner et al., 2010).

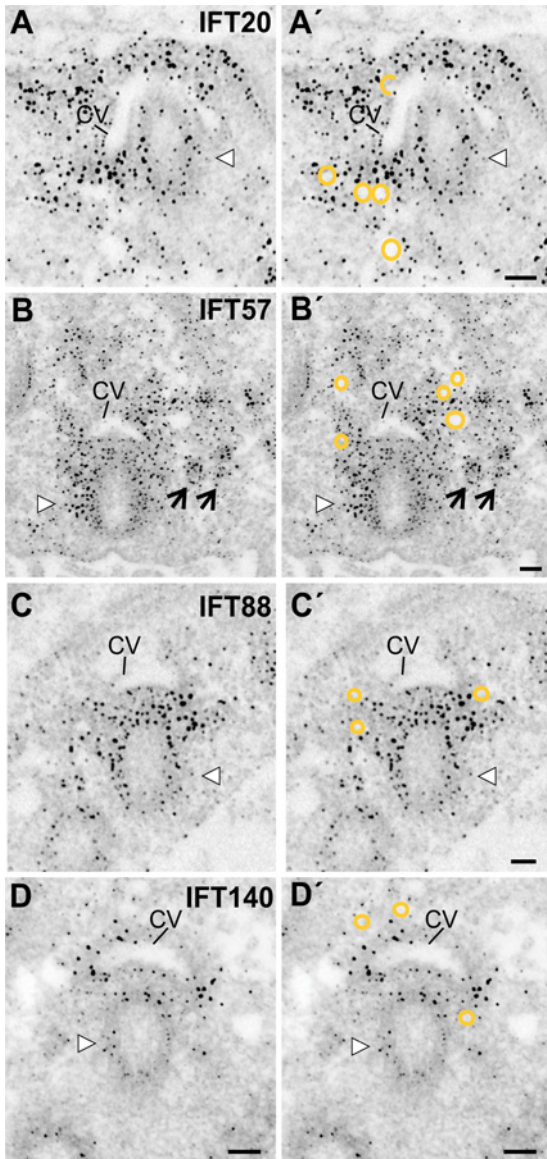
IFT molecules are involved in late stages of ciliogenesis

Our results demonstrate that IFT proteins are expressed during all stages of ciliogenesis in photoreceptor cells and are found within the differentiating photoreceptor ciliary shaft as soon as it appears (Figure 11). In the evolving ciliary shaft, the IFT proteins most probably participate in IFT processes. This indicates that IFT is required for the elongation of the differentiating cilium and assembly of the ciliary shaft and axoneme, confirming previous data (reviewed by Rosenbaum and Witman, 2002; Pedersen and Rosenbaum, 2008).

Interestingly, IFT20 appeared in the transition from stage S4 to S5 of rod photoreceptor ciliogenesis in the evolving ciliary shaft and in its distal swelling containing membrane vesicles of the premature outer segment. This is in contrast with our previous observations in mature photoreceptor cells in which IFT20 was absent from the connecting cilium and the axoneme (Sedmak and Wolfrum, 2010). Nevertheless,

Figure 7 | Association of IFT proteins with the ciliary vesicle and post-Golgi vesicles in early ciliogenesis stages of mouse photoreceptor cells

(A–D) Immunoelectron microscopic labelling of IFT proteins at the ciliary vesicle (CV), the basal body (white arrowhead) and post-Golgi vesicles indicated by orange circles in (A')–(D'). IFT57 is additionally detected in centriolar satellites (black arrows). Scale bars: 100 nm.



the association of IFT20 with membrane vesicles in the premature outer segment is consistent with the IFT20 localization at Golgi membranes and post-Golgi transport vesicles as shown previously (Folitt et al., 2006, 2008; Sedmak et al., 2009; Sedmak and

Wolfrum, 2010). We therefore speculate that IFT20 may play a role in the delivery of vesicles to differentiating membrane discs in the premature photoreceptor outer segment. In later stages of ciliogenesis, when the outer segment matures, membrane vesicles and IFT20 disappear from the outer segment base. A crucial role of IFT20 has been recently described for the formation of photoreceptor outer segments in knock-out (Keady et al., 2011), which is in line the present results on IFT20 in photoreceptor ciliogenesis.

In addition to their location in the ciliary shaft, all analysed IFT proteins were found at the ciliary base during later stages of photoreceptor ciliogenesis (Figure 11). There, the IFT proteins were present at the basal body, which is consistent with the observations for the ciliary region of the mature photoreceptor cell (Sedmak and Wolfrum, 2010). This pool of IFT proteins was previously judged to be involved in the assembly of IFT particles and the sorting of cargo for the delivery into the cilium (reviewed by Pedersen and Rosenbaum, 2008; Insinna and Besharse, 2008; Insinna et al., 2008, 2009; Pigino et al., 2009). Furthermore, in stages S3–S6, IFT20 and IFT52 were located in the apical periciliary extension of the differentiating inner segment. In mature photoreceptor cells this apical region was recently identified as a periciliary target area for post-Golgi transport vesicles containing cargo with a ciliary destination (Liu et al., 2007; Maerker et al., 2008; Sedmak and Wolfrum, 2010; Yang et al., 2010).

IFT proteins in early stages of intracellular ciliogenesis

We show for the first time that IFT proteins are expressed as early as PN0 in the apical part of the neuroblastic layer of the developing murine retina, which is in agreement with the localization of IFT52 and IFT88 in the developing zebra fish retina (Sukumaran and Perkins, 2009). Our correlated light and electron microscopy analyses demonstrated that, in the absence of any ciliary shaft, the IFT proteins are found at the daughter and mother centrioles. At these early stages, IFT proteins were also associated with the primary ciliary vesicle, centriolar satellites and post-Golgi vesicles in the cytoplasm of the neuroblasts of the developing retina (Figure 11).

As in mature primary cilia and photoreceptors, the prominent accumulation of IFT proteins in the periciliary cytoplasm at the base of the cilia most probably

Figure 8 | Immunoelectron microscopic localization of IFT proteins in stages S3 and S4 of photoreceptor cell ciliogenesis

(A–E) Immunoelectron labelling of IFT20, IFT52, IFT57, IFT88 and IFT140 in longitudinal and ciliary cross-sections of differentiating mouse photoreceptor cells. (F) Diagram of stages S3 and S4 of photoreceptor cell ciliogenesis. In S3 the photoreceptor inner segment (IS) extends and its protrusion, the apical IS, grows (dotted line); in S4 the elongating cilium (C) can be divided into a proximal (pC) and a distal cilium (dC) portion. (A–E) Antibodies to all IFT proteins are detected the basal body (white arrowhead) and the adjacent centriole (black arrowhead). IFT20, IFT52 and IFT57 are labelled in the apical inner segment (IS). IFT20 and IFT57 are detected at centriolar satellites (black arrow and grey circles in E). In contrast with IFT20, all other IFT proteins are found in C. IFT52 and IFT57 are also associated with the cytoplasm in the periphery of the basal body. IFT88 and IFT140 are additionally detected in the elongating ciliary shaft of the dC. Symbols '>' and '<', adherent junctions at the outer limiting membrane. Scale bars: (A, B, D and insets) 100 nm and (C, F) 200 nm.

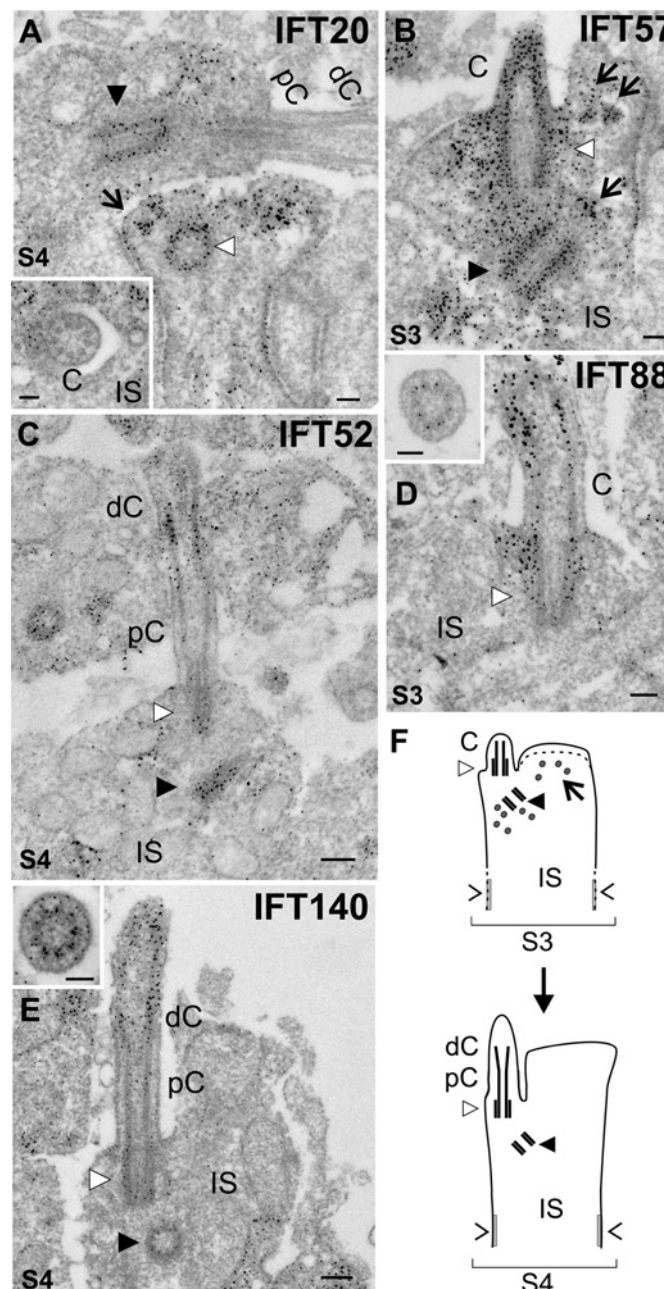


Figure 9 | Localization of IFT proteins in the basal part of the outer segment and at the basal body during late ciliogenesis of photoreceptor cells

(A–F) Immunoelectron microscopy of IFT52 (A, B), IFT57 (C), IFT88 (D, E) and IFT140 (F) in differentiating photoreceptor cells. (A–F) In S5 and S6 IFT52 is associated with the basal body (white arrowhead) and the distal part of the connecting cilium and present in the base (#) of the outer segment (OS). IFT57, IFT88 and IFT140 are located at the adjacent centriole (black arrowhead), at the basal body (white arrowhead), in the CC (cross-section) and at the OS base (#). IFT57 is not detected in the axoneme (white arrow). IFT88 and IFT140 labelling are present in the OS base (#) and extend further into the axoneme (white arrows). (G) Schema of ciliogenesis in stages S4–S6 of differentiating mouse photoreceptor cells. In stage S5 the proximal cilium (pC) becomes the connecting cilium (CC) and the distal cilium (dC) forms the outer segment (OS). Scale bars: 200 nm.

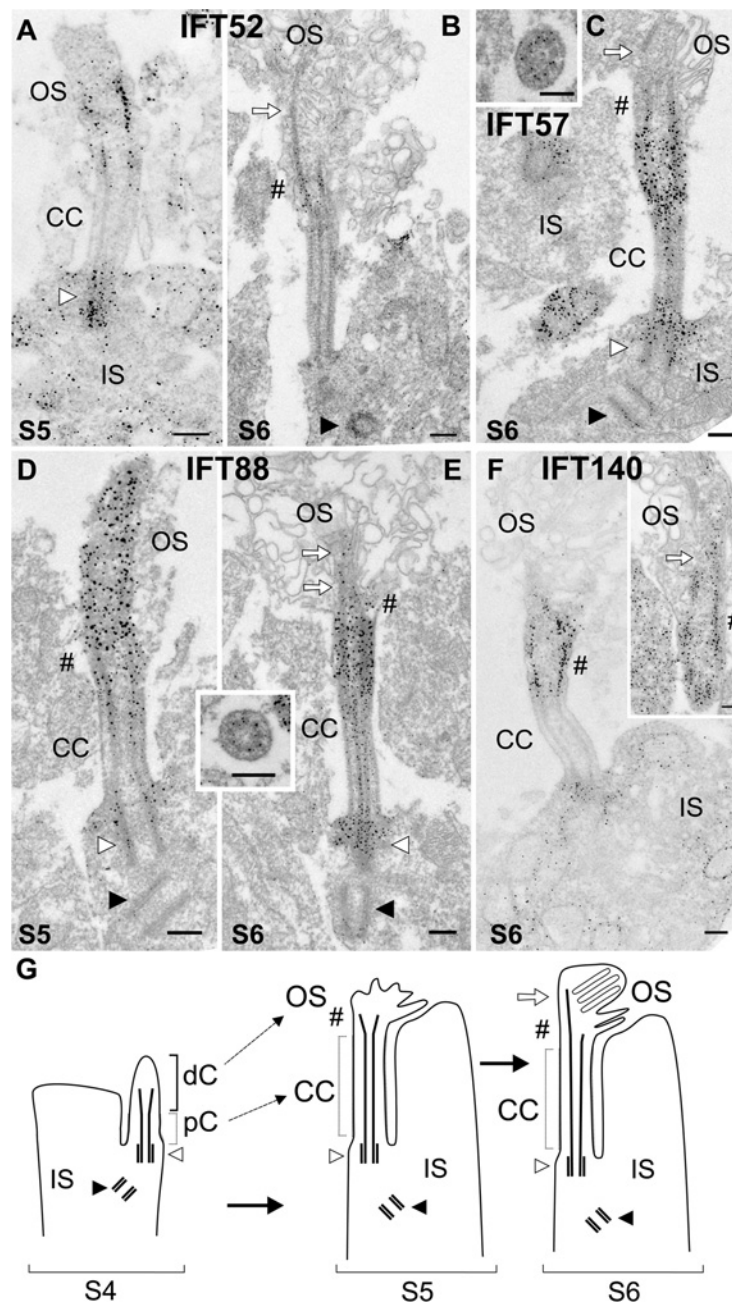


Figure 10 | Differential localization of IFT20 in the outgrowing cilium

(A–H) Immunoelectron localization of IFT20 in longitudinal and cross-sections (**B, E**) through differentiating mouse photoreceptor cells. **(I)** Diagram of ciliogenesis in stages S4–S6 of differentiating mouse photoreceptor cells. In S4 IFT20 is restricted to the basal body (white arrowhead), the adjacent centriole (black arrowhead) and the apical inner segment (IS) (asterisk). It is absent from the proximal (pC) and distal cilium (dC). **(C)** Between stage S4 and S5 IFT20 is concentrated at the basal body (white arrowhead) and the adjacent centriole (black arrowhead) and in the elongating cilium IFT20 is detected at the dC. **(D, E)** In S5 IFT20 is detected at the BB and at the basal outer segment (OS) (#), but in the axoneme (white arrow). **(F, G)** During S6 the OS formation proceeds and IFT20 is sporadically detected in the connecting cilium (CC) (indicated by double black arrowheads in **F**) and the base of OS (#). In mature photoreceptors IFT20 is concentrated in the apical IS (asterisk) and adjacent centriole, but absent from the CC. Scale bars: (**A–C, E, F**) 100 nm and (**D, G, H**) 200 nm.

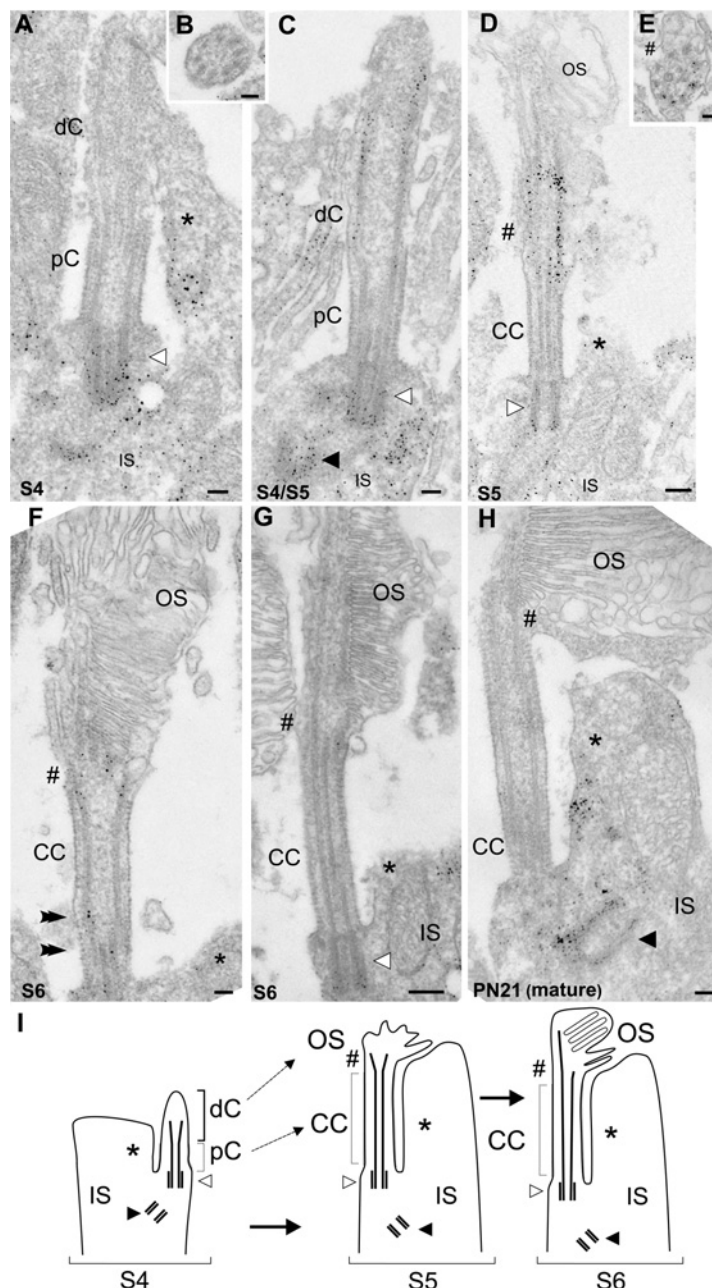
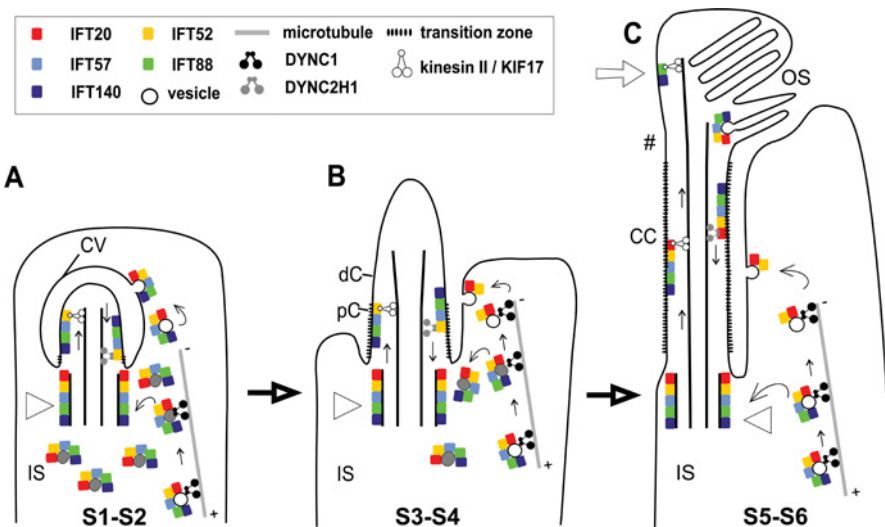


Figure 11 | Models of processes associated with IFT proteins during ciliogenesis in photoreceptor cells

The stages of ciliogenesis are characterized by different processes: **(A)** formation and expansion in S1–S2; **(B)** fusion of the ciliary vesicle with the apical plasma membrane (not shown), elongation of the ciliary bud and first IFT in the proximal cilium (pC) to the distal cilium (dC) in S3–S4; **(C)** outer segment (OS) formation and IFT through the connecting cilium (CC) and along axonemal microtubules (white arrow) in S5–S6. Present results further support the well-established participation of IFT proteins at the IFT processes in stages S3–S6 of photoreceptor ciliogenesis. At the OS base (#), most of the IFT proteins may dissociate from the cargo that is incorporated into OS disc membranes and used for the formation of photo-transductive OS disc membranes in stages S5 and S6. The temporary presence of IFT20 at the OS base (#) during the first stages of OS differentiation suggests that IFT20 may play a role at the initiation of the OS morphogenesis. Further apical in the OS, IFT particles containing IFT88 and IFT140 may participate at the transport processes along axonemal microtubules. However, during all stages the five investigated IFT proteins are associated with the mother centriole/basal body (white arrowhead), centriolar satellites (grey circles) and vesicles in the cytoplasm of the differentiating inner segment (IS) alluding to functions of IFT proteins different from IFT. Conclusively, these associations may indicate putative participation of IFT proteins at the transport of centriolar satellites (grey circles) containing non-membranous ciliary components and post-Golgi vesicles to the basal body (S1–S6). In S1–S2 the special distribution of IFT proteins at the ciliary vesicle and the cytoplasmic vesicles suggests a possible role of IFT proteins in ciliary vesicle formation and extension.



resembles a pool of IFT molecules that is stored for subsequent assembly of IFT complexes and IFT across the growing ciliary shaft in the later stages of ciliogenesis (Figure 11). However, since ciliary shaft does not exist in these differentiating stages, motile processes related to IFT are not occurring. Therefore we speculate that the cytoplasmic localization of IFT proteins in these early stages may indicate roles of IFT proteins beyond their well-established function for IFT in mature cilia and flagella. Interestingly, the IFT proteins were found in the cytoplasm in close proximity to centriolar satellites and post-Golgi vesicles (Figure 11), structures that are commonly thought to be involved in the delivery of ciliary components to the base of the cilium (Sorokin, 1962; Kubo et al.,

1999; Laoukili et al., 2000; Kubo and Tsukita, 2003; Moser et al., 2009). The present association of IFT proteins with post-Golgi transport vesicles during ciliogenesis agrees with data we have recently reported for IFT proteins in defined periciliary target domains for cytoplasmic transport in mature photoreceptor cells (Sedmak and Wolfrum, 2010). During early ciliogenesis IFT proteins may participate in conducting post-Golgi vesicles to the membrane of the ciliary vesicle for vesicle extension and for the delivery of ciliary membrane cargo to the elongating ciliary bud and shaft (Figure 11). These findings may further support the hypothesis that IFT proteins are evolutionarily related to proteins involved in exocytosis processes, in which post-Golgi vesicles fuse with the

IFT molecules in photoreceptor ciliogenesis

plasma membrane as previously suggested by Jekely and Arendt (2006).

In previous studies, several molecular compounds of centrosomes and basal bodies, for example the PCM-1 (pericentriolar material-1) protein, BBS4 (Bardet–Biedl syndrome protein 4), centrins, pericentrin and CEP290 (centrosomal protein 290) were found to be associated with the centriolar satellites (Kubo et al., 1999; Laoukili et al., 2000; Dammermann and Merdes, 2002; Kubo and Tsukita, 2003; Kim et al., 2004; Nachury et al., 2007; Kim et al., 2008). In these studies the localization of these centrosomal proteins at the centriolar satellites was interpreted as a possible role of these proteins in the transport of non-membrane associated ciliary cargo (e.g. α/β -tubulin dimers) to the basal body. Accordingly, we suggest a role of IFT proteins at the centriolar satellites in cargo transport to the ciliary base.

Our analyses of early ciliogenesis stages showed that the transition zone defines the boundary between the plasma membrane and the ciliary membrane already in the early stages of ciliogenesis. Although there is evidence that the doublet microtubules in the transition zone form independently of IFT (Rohatgi and Snell, 2010), we detected IFT proteins as soon as the transition zone appeared, even before the ciliary shaft extended. This observation raises the possibility that IFT proteins may play, in concert with characteristic transition zone molecules such as the recently identified microtubule–membrane linker CEP290 (Craigie et al., 2010), the ‘quality control’ function of the transition zone for ciliary cargo delivery. In any case, functional data obtained by knockout or knock-down experiments should provide further, more specific insights into the roles of IFT proteins during ciliogenesis.

Conclusions

In conclusion, the present study demonstrates that ciliogenesis in photoreceptor cells follows the intracellular ciliogenesis pathway, which can be divided into six distinct stages (S1–S6). The first stages (S1–S3) are characterized by electron-dense centriolar satellites and a ciliary vesicle, whereas the formation of the ciliary shaft and the light-sensitive outer segment discs are features of the three later stages. We provide evidence for the participation of IFT proteins already in early photoreceptor ciliogenesis before the

differentiating cilium emerges into the extracellular environment. IFT proteins localized in the periciliary cytoplasm at the base of the cilia may provide a pool of IFT molecules stored for the later delivery into the growing ciliary axoneme for IFT. However, the cytoplasmic localization of IFT proteins in the absence of a ciliary shaft in early stages of ciliogenesis may also suggest roles of IFT proteins beyond their well-established function in bidirectional ciliary transport recently reported (Finetti et al., 2009; Baldari and Rosenbaum 2010; Sedmak and Wolfrum, 2010).

Materials and methods

Animals

All experiments conformed to the guidelines provided by the ARVO (Association for Research in Vision and Ophthalmology) regarding the care and use of animals in research. C57BL/6J mice were maintained on a 12 h light/12 h dark cycle, with food and water *ad libitum*.

Antibodies and fluorescent dyes

Affinity-purified antibodies against individual IFT proteins (IFT20, IFT52, IFT57, IFT88 and IFT140) raised in rabbit were previously characterized (Pazour et al., 2002; Follit et al., 2006; Sedmak and Wolfrum, 2010). Monoclonal antibodies to centrin were used as a molecular marker for the ciliary apparatus of photoreceptors (Trojan et al., 2008). Secondary antibodies conjugated to Alexa Fluor[®] 488 or Alexa Fluor[®] 568 (Invitrogen, Karlsruhe, Germany) and biotinylated secondary antibodies (Vector Laboratories, Burlingame, CA, U.S.A.) were used. Nuclear DNA was stained by 1 $\mu\text{g}/\mu\text{l}$ of DAPI (4',6-diamidino-2-phenylindole; Sigma–Aldrich, Deisenhofen, Germany).

Immunofluorescence microscopy

Postnatal mouse eyes (PN0, PN3 and PN7) were enucleated and cryofixed in melting isopentane enclosed by liquid nitrogen and sectioned with a cryostat as described previously (Wolfrum, 1991). Cryosections were placed on poly-L-lysine-precoated coverslips, incubated with 0.01% Tween 20 in PBS and washed with PBS. Next, the cryosections were incubated with blocking solution (0.5% cold-water fish gelatine and 0.1% ovalbumin in PBS) for 1 h and with primary antibodies diluted in blocking solution at 4°C overnight. PBS-washed cryosections were incubated with Alexa Fluor[®] 488- or Alexa Fluor[®] 568-conjugated secondary antibodies in PBS with DAPI. For controls Alexa-conjugated secondary antibodies were omitted. Cryosections were mounted in Mowiol 4.88 (Hoechst, Frankfurt, Germany), analysed with a Leica DM 6000 B microscope (Leica, Wetzlar, Germany) through a $\times 63$ NA 1.32 HCX Plan-Apochromat and a $\times 100$ NA 1.4 Plan-Apochromat oil objective lens. Acquired images were processed with Adobe Photoshop CS (Adobe Systems, San Jose, CA, U.S.A.).

Conventional electron microscopy

For the ultrastructural analysis of the developing retina, enucleated eyes were fixed in 2.5% glutaraldehyde in 0.1 M cacodylate buffer containing 0.1 M sucrose for 1.5 h at 4°C. After 30 min of this fixation the cornea and lens were removed to obtain an eye cup, which was further fixed for another 1 h. After this fixation step, eye cups were washed with 0.1 M cacodylate buffer containing 0.1 M sucrose for 30 min. Subsequently, eye cups were fixed with 2% osmium tetroxide (OsO₄) in 0.1 M cacodylate buffer containing 0.1 M sucrose for 1 h at room temperature. After this second fixation step, specimens were dehydrated in ethanol (30–100%) and embedded in Renlam[®] M-1 resin (Serva Electrophoresis, Heidelberg, Germany).

Immunoelectron microscopy: pre-embedding labelling

For immunoelectron microscopy, a previously described protocol of pre-embedding labelling was applied (Maerker et al., 2008; Sedmak et al., 2009). In short, during pre-fixation of isolated mouse eyes in 4% (w/v) paraformaldehyde in Soerensen buffer (0.1 M Na₂HPO₄·2H₂O and 0.1 M KH₂PO₄, pH 7.4), eyes were perforated with a needle and lenses with corneas were removed. Washed retinas were dissected and infiltrated with 10 and 20% sucrose in Soerensen buffer, followed by 30% sucrose overnight. After four cycles of freezing in liquid nitrogen and thawing at 37°C, retinas were washed in PBS and embedded in buffered 2% agar (Sigma–Aldrich). Agar blocks were sectioned in 50 µm sections with a vibratome (Leica VT 1000 S). For suppressing endogenous peroxidase activity, vibratome sections were incubated with 3% H₂O₂ for 10 min. Subsequently, the sections were kept in 10% (v/v) normal goat serum and 1% BSA in PBS and incubated with primary antibodies against IFT proteins for 4 days at 4°C. PBS-washed sections were incubated with the appropriate biotinylated secondary antibodies, which were visualized using a Vectastain ABC kit (Vector Laboratories). To maintain the staining, retina sections were fixed in 2.5% glutaraldehyde in 0.1 M cacodylate buffer (pH 7.4). Further, diaminobenzidine precipitates were silver-enhanced and post-fixed in 0.5% OsO₄ in 0.1 M cacodylate buffer on ice. Dehydrated specimens were flat-mounted between ACLAR[®] films (Ted Pella, Redding, CA, U.S.A.) in Renlam[®] M-1 resin.

Ultrathin sectioning and transmission electron microscopy

Ultrathin sections were made using a Reichert Ultracut S ultramicrotome (Leica), collected on Formvar-coated copper grids and counterstained with heavy metal staining (2% uranyl acetate in 50% ethanol; aq. 2% lead citrate). Ultrathin sections were analysed in a Tecnai 12 BioTwin transmission electron microscope (FEI, Eindhoven, The Netherlands). Images were obtained with a CCD camera (charge-coupled-device camera; SIS MegaView3; Surface Imaging Systems, Herzogenrath, Germany) and processed with Adobe Photoshop CS (Adobe Systems).

Author contribution

Tina Sedmak performed all the experiments, wrote the first draft of the manuscript and contributed to the design of the experiments. Uwe Wolfrum

mainly conceived this study. Both authors contributed to the final version of the manuscript.

Acknowledgements

We thank E. Sehn for excellent technical assistance and Dr A. Giessl, Dr H. Regus-Leidig and Dr M. van Wyk, as well as N. Overlack and N. Sorousch, for discussions and a critical reading of the paper prior to submission.

Funding

The work was supported by the Deutsche Forschungsgemeinschaft [grant number GRK1044 (to U.W.)]; the European Community FP7/2009 [grant number 241955, SYSCILIA (to U.W.)]; and the FAUN-Stiftung, Nuremberg (to U.W.). T.S. was supported by a stipend from the Rheinland-Pfalz Graduiertenförderung.

References

- Badano, J.L., Mitsuma, N., Beales, P.L. and Katsanis, N. (2006) The ciliopathies: an emerging class of human genetic disorders. *Annu. Rev. Genomics Hum. Genet.* **7**, 125–148
- Baker, K. and Beales, P.L. (2009) Making sense of cilia in disease: the human ciliopathies. *Am. J. Med. Genet. C. Semin. Med. Genet.* **151C**, 281–295
- Baldari, C.T. and Rosenbaum, J. (2010) Intraflagellar transport: it's not just for cilia anymore. *Curr. Opin. Cell Biol.* **22**, 75–80
- Besharse, J.C., Horst, C.J. (1990) The photoreceptor connecting cilium – a model for the transition zone. In *Ciliary and Flagellar Membranes* (Bloodgood, R.A., ed.), pp. 389–417, Plenum, New York
- Carter-Dawson, L.D. and LaVail, M.M. (1979) Rods and cones in the mouse retina. I. Structural analysis using light and electron microscopy. *J. Comp. Neurol.* **188**, 245–262
- Chaitin, M.H. (1992) Double immunogold localization of opsin and actin in the cilium of developing mouse photoreceptors. *Exp. Eye Res.* **54**, 261–267
- Craige, B., Tsao, C.C., Diener, D.R., Hou, Y., Lechtreck, K.F., Rosenbaum, J.L. and Witman, G.B. (2010) CEP290 tethers flagellar transition zone microtubules to the membrane and regulates flagellar protein content. *J. Cell Biol.* **190**, 927–940
- Cole, D.G. (2003) The intraflagellar transport machinery of *Chlamydomonas reinhardtii*. *Traffic* **4**, 435–442
- Cole, D.G., Diener, D.R., Himelblau, A.L., Beech, P.L., Fuster, J.C. and Rosenbaum, J.L. (1998) *Chlamydomonas* kinesin-II-dependent intraflagellar transport (IFT): IFT particles contain proteins required for ciliary assembly in *Caenorhabditis elegans* sensory neurons. *J. Cell Biol.* **141**, 993–1008
- Dammermann, A. and Merdes, A. (2002) Assembly of centrosomal proteins and microtubule organization depends on PCM-1. *J. Cell Biol.* **159**, 255–266
- Finetti, F., Paccani, S.R., Riparbelli, M.G., Giacomello, E., Perinetti, G., Pazour, G.J., Rosenbaum, J.L. and Baldari, C.T. (2009) Intraflagellar transport is required for polarized recycling of the TCR/CD3 complex to the immune synapse. *Nat. Cell Biol.* **11**, 1332–1339

- Follitt, J.A., Tuft, R.A., Fogarty, K.E. and Pazour, G.J. (2006) The intraflagellar transport protein IFT20 is associated with the Golgi complex and is required for cilia assembly. *Mol. Biol. Cell* **17**, 3781–3792
- Follitt, J.A., San Agustin, J.T., Xu, F., Jonassen, J.A., Samtani, R., Lo, C.W. and Pazour, G.J. (2008) The golgin GMAP210/TRIP11 anchors IFT20 to the golgi complex. *PLoS Genet.* **4**, e1000315, doi:10.1371/journal.pgen.1000315
- Gerdes, J.M., Davis, E.E. and Katsanis, N. (2009) The vertebrate primary cilium in development, homeostasis, and disease. *Cell* **137**, 32–45
- Ghossoub, R., Molla-Herman, A., Bastin, P. and Benmerah, A. (2011) The ciliary pocket: a once-forgotten membrane domain at the base of cilia. *Biol. Cell* **103**, 131–144
- Gilula, N.B. and Satir, P. (1972) The ciliary necklace. A ciliary membrane specialization. *J. Cell Biol.* **53**, 494–509
- Goetz, S.C. and Anderson, K.V. (2010) The primary cilium: a signalling centre during vertebrate development. *Nat. Rev. Genet.* **11**, 331–344
- Greiner, J.V., Weidman, T.A., Bodley, H.D. and Greiner, C.A. (1981) Ciliogenesis in photoreceptor cells of the retina. *Exp. Eye Res.* **33**, 433–446
- Hames, R.S., Crookes, R.E., Straatman, K.R., Merdes, A., Hayes, M.J., Faragher, A.J. and Fry, A.M. (2005) Dynamic recruitment of Nek2 kinase to the centrosome involves microtubules, PCM-1, and localized proteasomal degradation. *Mol. Biol. Cell* **16**, 1711–1724
- Insinna, C. and Besharse, J.C. (2008) Intraflagellar transport and the sensory outer segment of vertebrate photoreceptors. *Dev. Dyn.* **237**, 1982–1992
- Insinna, C., Pathak, N., Perkins, B., Drummond, I. and Besharse, J.C. (2008) The homodimeric kinesin, Kif17, is essential for vertebrate photoreceptor sensory outer segment development. *Dev. Biol.* **316**, 160–170
- Insinna, C., Humby, M., Sedmak, T., Wolfrum, U. and Besharse, J.C. (2009) Different roles for KIF17 and kinesin II in photoreceptor development and maintenance. *Dev. Dyn.* **238**, 2211–2222
- Jekely, G. and Arendt, D. (2006) Evolution of intraflagellar transport from coated vesicles and autogenous origin of the eukaryotic cilium. *BioEssays* **28**, 191–198
- Jeon, C.J., Strettoi, E. and Masland, R.H. (1998) The major cell populations of the mouse retina. *J. Neurosci.* **18**, 8936–8946
- Keady, B.T., Le, Y.Z. and Pazour, G.J. (2011) IFT20 is required for opsin trafficking and photoreceptor outer segment development. *Mol. Biol. Cell* **22**, 921–930
- Kim, J.C., Badano, J.L., Sibold, S., Esmail, M.A., Hill, J., Hoskins, B.E., Leitch, C.C., Venner, K., Ansley, S.J., Ross, A.J. et al. (2004) The Bardet–Biedl protein BBS4 targets cargo to the pericentriolar region and is required for microtubule anchoring and cell cycle progression. *Nat. Genet.* **36**, 462–470
- Kim, J., Krishnaswami, S.R. and Gleeson, J.G. (2008) CEP290 interacts with the centriolar satellite component PCM-1 and is required for Rab8 localization to the primary cilium. *Hum. Mol. Genet.* **17**, 3796–3805
- Kim, J., Lee, J.E., Heynen-Genel, S., Suyama, E., Ono, K., Lee, K., Ideker, T., za-Blanc, P. and Gleeson, J.G. (2010) Functional genomic screen for modulators of ciliogenesis and cilium length. *Nature* **464**, 1048–1051
- Krock, B.L. and Perkins, B.D. (2008) The intraflagellar transport protein IFT57 is required for cilia maintenance and regulates IFT-particle-kinesin-II dissociation in vertebrate photoreceptors. *J. Cell Sci.* **121**, 1907–1915
- Krock, B.L., Mills-Henry, I. and Perkins, B.D. (2009) Retrograde intraflagellar transport by cytoplasmic dynein-2 is required for outer segment extension in vertebrate photoreceptors but not arresting translocation. *Invest. Ophthalmol. Vis. Sci.* **50**, 5463–5471
- Kubo, A. and Tsukita, S. (2003) Non-membranous granular organelle consisting of PCM-1: subcellular distribution and cell-cycle-dependent assembly/disassembly. *J. Cell Sci.* **116**, 919–928
- Kubo, A., Sasaki, H., Yuba-Kubo, A., Tsukita, S. and Shiina, N. (1999) Centriolar satellites: molecular characterization, ATP-dependent movement toward centrioles and possible involvement in ciliogenesis. *J. Cell Biol.* **147**, 969–980
- Laoukili, J., Perret, E., Middendorp, S., Houcine, O., Guennou, C., Marano, F., Bornens, M. and Tournier, F. (2000) Differential expression and cellular distribution of centrin isoforms during human ciliated cell differentiation *in vitro*. *J. Cell Sci.* **113**, 1355–1364
- LaVail, M.M. (1973) Kinetics of rod outer segment renewal in the developing mouse retina. *J. Cell Biol.* **58**, 650–661
- Livesey, F.J. and Cepko, C.L. (2001) Vertebrate neural cell-fate determination: lessons from the retina. *Nat. Rev. Neurosci.* **2**, 109–118
- Liu, Q., Tan, G., Levenkova, N., Li, T., Pugh, Jr, E.N., Rux, J.J., Speicher, D.W. and Pierce, E.A. (2007) The proteome of the mouse photoreceptor sensory cilium complex. *Mol. Cell. Proteomics* **6**, 1299–1317
- Maerker, T., van Wijk, E., Overlack, N., Kersten, F.F., McGee, J., Goldmann, T., Sehn, E., Roepman, R., Walsh, E.J., Kremer, H. and Wolfrum, U. (2008) A novel Usher protein network at the periciliary reloading point between molecular transport machineries in vertebrate photoreceptor cells. *Hum. Mol. Genet.* **17**, 71–86
- Molla-Herman, A., Ghossoub, R., Blisnick, T., Meunier, A., Serres, C., Silbermann, F., Emmerson, C., Romeo, K., Bourdoncle, P., Schmitt, A. et al. (2010) The ciliary pocket: an endocytic membrane domain at the base of primary and motile cilia. *J. Cell Sci.* **123**, 1785–1795
- Moser, J.J., Fritzler, M.J. and Rattner, J.B. (2009) Primary ciliogenesis defects are associated with human astrocytoma/glioblastoma cells. *BMC Cancer* **9**, 448
- Murcia, N.S., Richards, W.G., Yoder, B.K., Mucenski, M.L., Dunlap, J.R. and Woychik, R.P. (2000) The Oak Ridge Polycystic Kidney (orpk) disease gene is required for left-right axis determination. *Development* **127**, 2347–2355
- Nachury, M.V., Loktev, A.V., Zhang, Q., Westlake, C.J., Peranen, J., Merdes, A., Slusarski, D.C., Scheller, R.H., Bazan, J.F., Sheffield, V.C. and Jackson, P.K. (2007) A core complex of BBS proteins cooperates with the GTPase Rab8 to promote ciliary membrane biogenesis. *Cell* **129**, 1201–1213
- Nir, I., Cohen, D. and Papermaster, D.S. (1984) Immunocytochemical localization of opsin in the cell membrane of developing rat retinal photoreceptors. *J. Cell Biol.* **98**, 1788–1795
- Omori, Y., Zhao, C., Saras, A., Mukhopadhyay, S., Kim, W., Furukawa, T., Sengupta, P., Veraksa, A. and Malicki, J. (2008) Eilpsa is an early determinant of ciliogenesis that links the IFT particle to membrane-associated small GTPase Rab8. *Nat. Cell Biol.* **10**, 437–444
- Pazour, G.J. and Bloodgood, R.A. (2008) Targeting proteins to the ciliary membrane. *Curr. Top. Dev. Biol.* **85**, 115–149
- Pazour, G.J., Baker, S.A., Deane, J.A., Cole, D.G., Dickert, B.L., Rosenbaum, J.L., Witman, G.B. and Besharse, J.C. (2002) The intraflagellar transport protein, IFT88, is essential for vertebrate photoreceptor assembly and maintenance. *J. Cell Biol.* **157**, 103–113
- Pedersen, L.B. and Rosenbaum, J.L. (2008) Intraflagellar transport (IFT) role in ciliary assembly, resorption and signalling. *Curr. Top. Dev. Biol.* **85**, 23–61
- Pedersen, L.B., Veland, I.R., Schroder, J.M. and Christensen, S.T. (2008) Assembly of primary cilia. *Dev. Dyn.* **237**, 1993–2006
- Pigino, G., Geimer, S., Lanzavecchia, S., Paccagnini, E., Cantele, F., Diener, D.R., Rosenbaum, J.L. and Lupetti, P. (2009) Electron-tomographic analysis of intraflagellar transport particle trains *in situ*. *J. Cell Biol.* **187**, 135–148

- Rattner, J.B., Sciore, P., Ou, Y., van der Hoorn, F.A. and Lo, I.K. (2010) Primary cilia in fibroblast-like type B synoviocytes lie within a cilium pit: a site of endocytosis. *Histol. Histopathol.* **25**, 865–875
- Roepman, R., Wolfrum, U. (2007) Protein networks and complexes in photoreceptor cilia. In *Subcellular Proteomics – From Cell Deconstruction to System Reconstruction* (Faupel, M. and Bertrand, E., eds), pp. 209–235, Springer, Dordrecht, The Netherlands
- Rohatgi, R. and Snell, W.J. (2010) The ciliary membrane. *Curr. Opin. Cell Biol.* **22**, 541–546
- Rosenbaum, J.L. and Witman, G.B. (2002) Intraflagellar transport. *Nat. Rev. Mol. Cell Biol.* **3**, 813–825
- Sedmak, T. and Wolfrum, U. (2010) Intraflagellar transport molecules in ciliary and nonciliary cells of the retina. *J. Cell Biol.* **189**, 171–186
- Sedmak, T., Sehn, E. and Wolfrum, U. (2009) Immunoelectron microscopy of vesicle transport to the primary cilium of photoreceptor cells. *Methods Cell Biol.* **94**, 259–272
- Sung, C.H. and Chuang, J.Z. (2010) The cell biology of vision. *J. Cell Biol.* **190**, 953–963
- Sorokin, S. (1962) Centrioles and the formation of rudimentary cilia by fibroblasts and smooth muscle cells. *J. Cell Biol.* **15**, 363–377
- Sorokin, S.P. (1968) Reconstructions of centriole formation and ciliogenesis in mammalian lungs. *J. Cell Sci.* **3**, 207–230
- Sukumaran, S. and Perkins, B.D. (2009) Early defects in photoreceptor outer segment morphogenesis in zebra fish *ift57*, *ift88* and *ift172* intraflagellar transport mutants. *Vision Res.* **49**, 479–489
- tom Dieck, S. and Brandstätter, J.H. (2006) Ribbon synapses of the retina. *Cell Tissue Res.* **326**, 339–346
- Trojan, P., Krauss, N., Choe, H.W., Giessl, A., Pulvermuller, A. and Wolfrum, U. (2008) Centrioles in retinal photoreceptor cells: regulators in the connecting cilium. *Prog. Retin. Eye Res.* **27**, 237–259
- Tokuyasu, K. and Yamada, E. (1959) The fine structure of the retina studied with the electron microscope. IV. Morphogenesis of outer segments of retinal rods. *J. Biophys. Biochem. Cytol.* **6**, 225–230
- Tsujikawa, M. and Malicki, J. (2004) Intraflagellar transport genes are essential for differentiation and survival of vertebrate sensory neurons. *Neuron* **42**, 703–716
- Wolfrum, U. (1991) Tropomyosin is co-localized with the actin filaments of the scolopale in insect sensilla. *Cell Tissue Res.* **265**, 11–17
- Yang, J., Liu, X., Zhao, Y., Adamian, M., Pawlyk, B., Sun, X., McMillan, D.R., Liberman, M.C. and Li, T. (2010) Ablation of whirlin long isoform disrupts the USH2 protein complex and causes vision and hearing loss. *PLoS Genet.* **6**, e1000955

Received 18 March 2011/10 June 2011; accepted 6 July 2011

Published as Immediate Publication 6 July 2011, doi:10.1042/BC20110034



Supplementary online data

Intraflagellar transport proteins in ciliogenesis of photoreceptor cells

Tina Sedmak¹ and Uwe Wolfrum²

Department of Cell and Matrix Biology, Institute of Zoology, Johannes Gutenberg University, Mainz, Germany

Supplementary Figures S1–S3 are on the following pages.

¹Present address: Department of Biology, Animal Physiology, University of Erlangen-Nuremberg, D-91058 Erlangen, Germany.

²To whom correspondence should be addressed (email wolfrum@uni-mainz.de).

Figure S1 | Expression of IFT proteins in the developing mouse retina

DAPI staining of nuclear DNA (left panel) and indirect immunofluorescence labelling of IFT20, IFT52, IFT57, IFT88 and IFT140 in cryosections through the developing retina of PN0, PN3 and PN7 mice. At PN0 and PN3 IFT proteins are mainly detected in the apical region of the neuroblastic layer (NBL). At PN7 IFT proteins are concentrated in the ciliary region (white double arrowhead) of photoreceptor cells. White asterisk indicates the outer plexiform layer; INL, the inner nuclear layer; OS, the outer segment; RPE, retinal pigment epithelium; GCL, ganglion cell layer. Scale bars, 10 μm .

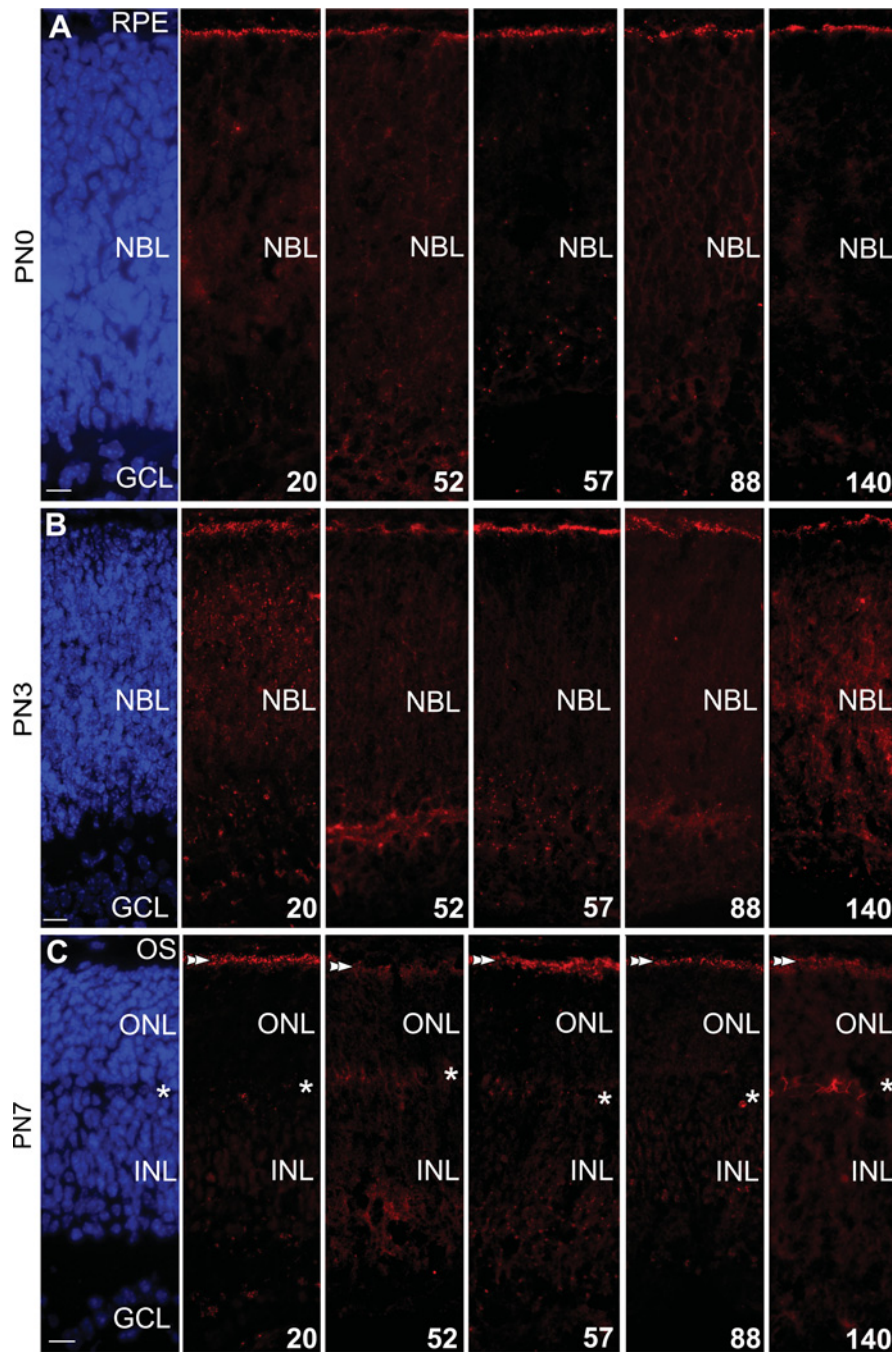
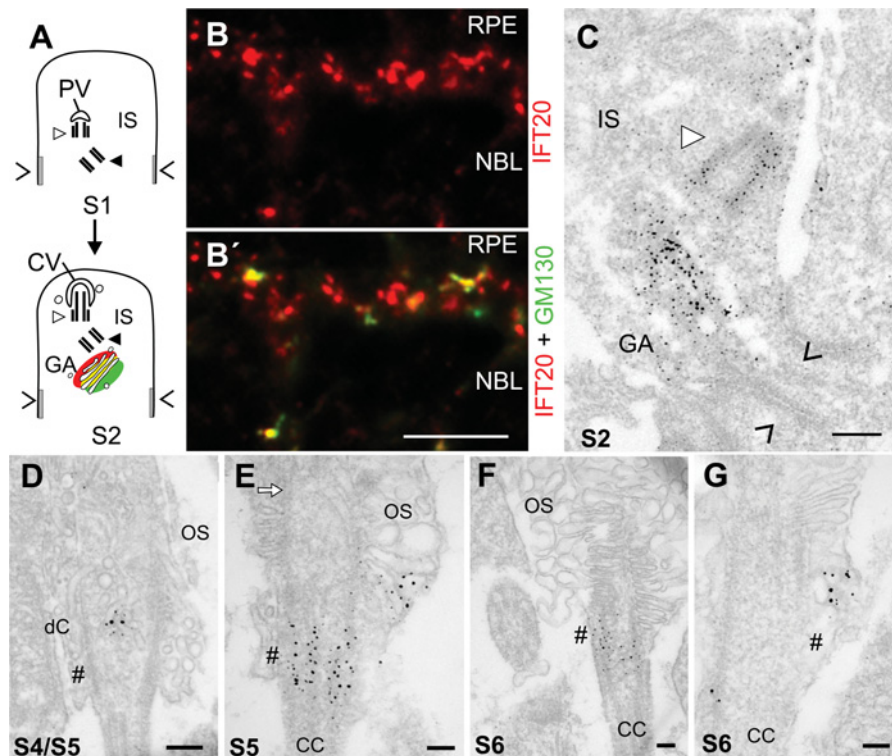


Figure S3 | Subcellular localization of IFT20 at the Golgi apparatus and in the cilium of the differentiating mouse photoreceptor cells

(A–C) Indirect immunofluorescence (B) by antibodies to IFT20 (red) and GM130 (Golgi matrix protein 130; green; merged in B') and immunoelectron microscopic (C) labelling of IFT20 at the Golgi apparatus (GA) illustrated in schematic representation (A). Double labelling of IFT20 and GM130 indicates partial co-localization in the apical part of the neuroblastic layer (NBL). Basal body is indicated by white arrowhead and adherent junctions by '>' and '<'. (D–G) Immunoelectron microscopic localization of IFT20 during late stages of photoreceptor cell ciliogenesis. In S4/S5, IFT20 is detected by a few particles in the distal connecting cilium (dC), whereas in S5 and S6 intense IFT20 labelling is observed at the base of the outer segment (#, OS). In S6, IFT20 is detected by a few particles in the connecting cilium (CC). In all stages IFT20 is absent from the axoneme (white arrow). IS, inner segment; RPE, retinal pigment epithelium. Scale bars: (B, B') 5 μ m; (C, D) 200 nm; (E–G) 100 nm.



Received 18 March 2011/10 June 2011; accepted 6 July 2011

Published as Immediate Publication 6 July 2011, doi:10.1042/BC20110034